

# Wettability Alteration in Near-Wellbore Regions of Gas Reservoirs to Mitigate Liquid Blockage Using Super Water- and Oil-Repellent ZnO/SiO<sub>2</sub> Nanofluid Treatment

- Pouriya Esmailzadeh, Mohammad Taghi Sadeghi\*  
Chemical Engineering College, Iran University of Science and Technology (IUST), Narmak, Tehran 16765-163, Iran  
\* (E-mail: sadeghi@iust.ac.ir)
- Alireza Bahramian  
Institute of Petroleum Engineering, University of Tehran, Iran

Received: Nov 29, 2016/ Revised: Dec 15, 2016 / Accepted: March 6, 2017

## Abstract

In gas-condensate reservoirs as the bottom hole pressure drops below the hydrocarbon dew point of the reservoir fluid, liquids drop out from the gas phase and establish condensate banking near the wellbore, resulting in lower gas productivity. Changing the reservoir rock wettability from liquid-wetting to gas-wetting has outstanding potential in improving the productivity of gas wells. In this work, we report the highly water- and oil-repellent properties of carbonate reservoir rocks treated with a nanofluid based on synthesized ZnO/SiO<sub>2</sub> nanocomposites and fluoro-containing materials PTFE, TFE, and PFOS. Carbonate plates coated with the prepared nanofluid exhibits a high contact angle of 162° for brine (contact angle hysteresis=0° and roll-off angle <2°), together with 135° for liquid gas-condensate, supporting significant super-amphiphobicity with self-cleaning properties. Surface characterization of the rock using SEM, SP, and EDX analyses reveals that the rough morphology of ZnO/SiO<sub>2</sub> nanocomposites combined with low surface energy of fluorochemical provides the surface superamphiphobicity. Moreover, the efficiency of the nanofluid in wettability alteration of carbonate core from liquid-wetting to ultra gas-wetting under reservoir conditions was investigated by performing gas/liquid two-phase flow tests with single-phase liquid-injection into the gas-saturated core. The results indicate that the mobility of liquid for both gas/brine and gas/liquid-condensate systems increases significantly after wettability alteration.

**Keywords:** Gas-wetness; Wettability alteration; Nanofluid; ZnO/SiO<sub>2</sub> nanocomposites; Gas condensate reservoir; liquid-repellent.

## 1. Introduction

Gas-condensate reservoirs experience a significant loss in well productivity as reservoir pressure drops below the hydrocarbon dew point owing to condensate banking in the near-wellbore region and subsequent reduction in gas relative permeability [1,2]. Water blocking also decreases the relative permeability of gas [2,3] and increases the impact of liquid blockage on lowering the gas well deliverability. A major factor in liquid accumulation is the low mobility of liquids due to strong liquid-wetting of the reservoir rock. Through wettability alteration of the rock from liquid-wetting to gas-wetting, the mobility of liquid phase for a gas/liquid system increases dominantly, preventing the liquid accumulation in high saturation and resulting in elevated gas production rates. The principal requirement is the permanent alteration of wettability to gas-wetting. Li and Firoozabadi were the first who demonstrated both theoretically [4] and experimentally [5] that the approach of wettability alteration to gas-wetting is promisingly effective for improving the productivity in gas-liquid systems. In the theoretical work, they studied the relative permeability of gas and liquid phase using a phenomenological network model. Their results showed that substantial increase in gas well deliverability may be obtained when the wettability of porous media alters to gas-wetting and is the most effective approach. They moreover showed experimentally that the oil recovery and phase relative permeability in gas/oil system can be increased by wettability alteration of rock to preferential gas-wetting using fluoro-polymer chemicals. Later many other researchers investigated experimentally the efficiency of various fluorochemical polymers/surfactants on changing the wettability of different rock types to gas-wetting [6-14]. However, some of these chemicals fail to be utilized for field applications because they were not cost-effective, environmentally friendly or losing their effectiveness under reservoir conditions.

Nanofluids are a new class of solid/liquid mixtures engineered by dispersing nanometer-size particles or any nanostructures in conventional base liquids [15,16]. Over the past decade, the innovative concept of nanofluids, as a part of nanotechnology, has developed largely and used in various industrial and biological processes, such as drug delivery [17], surface coating [18], heat transfer [19], environmental remediation [20], etc. [16,21]. Nanofluids also revealed their potential applications in oil and gas industries through wettability alteration of reservoir rock [22], enhanced oil recovery (EOR) process [23,24], drilling technology [25], reservoir exploration, and natural gas transportation [26,27].

Recently, few papers have been published that report the impact of silica based nanofluids which are capable of altering the wettability of rock towards gas-wetting [28,29]. Although their studies were promising, they have not succeeded to change the wettability of reservoir rock to ultra gas-wetting state; hence, the issue is still an ongoing field of research.

In this paper, It is revealed report the super water- and oil-repellent properties of a novel ZnO/SiO<sub>2</sub>-based nanofluid, applied to alter the wettability of a carbonate reservoir rock to ultra gas-wetting state. We verified the change of wettability by measuring contact angle and characterizing the rock surface using SEM images, EDX, and SP analyses. In continue, we investigate the practical efficiency of the superamphiphobic nanofluid in flow tests which represents better the reservoir conditions, by conducting a set of coreflooding experiments. Accordingly, the changes in the pressure drop and the liquid permeability in two-phase (gas/oil or gas/water) flow tests using single-phase liquid-injection into a gas-saturated core are measured before and after wettability alteration. It can be concluded believe that the novel formulated ZnO/SiO<sub>2</sub> nanofluid can improve the productivity of the reservoirs and mitigate water and condensate blockage in gas wells.

## 2. Materials and methods

### 2.1. Preparation of super liquid-repellent ZnO/SiO<sub>2</sub> nanofluid

In order to prepare the nanofluid, as a first step ZnO/SiO<sub>2</sub> nanocomposites were synthesized via wet-chemical co-precipitation method through a hydrothermal process. Accordingly, 0.02 mol of Zinc nitrate hexahydrate (Zn(NO<sub>3</sub>)<sub>2</sub>·6H<sub>2</sub>O, 98%, Merck) and 0.08 mol tetraethyl orthosilicate (TEOS, Si(OC<sub>2</sub>H<sub>5</sub>)<sub>4</sub>, 95%, Merck) were dissolved in water/isopropyl alcohol (C<sub>3</sub>H<sub>8</sub>O, Merck) solution and stirred magnetically for 15 min. then 10 g of acetylacetone (C<sub>5</sub>H<sub>8</sub>O<sub>2</sub>, >99%, Merck) dissolved in water/isopropyl alcohol solution and 20 g of oleic acid (C<sub>18</sub>H<sub>34</sub>O<sub>2</sub>, Merck) were added gently to the basic solution and hydrolyzed by addition of sodium hydroxide (NaOH, Merck)/water-ethanol solution in a dropwise manner, under vigorous stirring to obtain a mixture with pH of 10-11. After refluxing for 1 h at 80-90 °C, the prepared mixture was quenched rapidly for 45 min and then dried hydrothermally in an oven for 72 h at 90 °C. Next, it was filtered, washed with water and alcohol solution and then dried. The resultant product was finally calcined in a furnace in 3 steps at 200-900 °C for 10 h. This procedure results in achieving fine hydrophobic ZnO/SiO<sub>2</sub> nanocomposites.

Super water- and oil-repellent ZnO/SiO<sub>2</sub> nanofluid was fabricated by using of the synthesized nanocomposites and fluorochemicals. For this purpose, ZnO/SiO<sub>2</sub> nanocomposites, polytetrafluoroethylene (PTFE, Sigma-Aldrich), 2,2,2-Trifluoroethanol (TFE, SDFCL Co., 99%), ethanol and a mixture containing Trichloro(1H,1H,2H,2H-perfluorooctyl) silane (PFOS, 97%, Sigma-Aldrich) were dissolved with mass ratio of 0.002:0.2:0.003:1:1 at room temperature. Using ultrasonic bath, the resultant solution was sonicated then for 30-40 min, followed by 1 h agitation on a magnetic stirrer at 50 °C [30,31].

### 2.2. Porous medium and fluids

A cylindrical carbonate reservoir core with a length of 6 cm, the diameter of 3.8 cm and porosity of 20.7% used in this work to perform

core displacement tests. Static and dynamic contact angle measurements were also done on small circular rock plates that have been taken from a similar large slab of this carbonate reservoir core, respectively.

The plates and core being subjected to different tests, they were cleaned in Soxhlet extraction apparatus where they were flushed with toluene and methanol for 24 and 72 h, respectively. The pre-treatment process was followed by drying of rock in an oven at 80 °C for 24 h.

Distilled water and 2 wt% NaCl brine were used as the aqueous phase in order to investigate the hydrophobicity of rocks. Normal decane (C<sub>10</sub>H<sub>22</sub>, Merck, >99%) and a gas-condensate liquid sample from an Iranian gas condensate reservoir were used as the oil phase to study the oleophobicity of rocks. At 25 °C, the gas-condensate sample has a specific gravity of 0.78 and a viscosity of 1.28 cP. Air and nitrogen were also used as the gas phase in contact angle measurements and core displacement tests, respectively.

### 2.3. Treatment process

#### 2.3.1. Contact angle tests

The clean and dry carbonate rock plates were totally submerged in fabricated nanofluid and aged in an oven at 80 °C for 48 h to let the nanocomposites and fluoro-containing materials sediment on the surface of plates and create a liquid-repellent layer on them. Next, the plates were removed from the nanofluid and dried in an oven at 80 °C and finally the dried plates were subjected to the contact angle measurement test.

#### 2.3.2. Core displacement tests

In order to change the wettability of the core to gas-wetting state, it was put in a coreflooding apparatus, which is capable of resisting reservoir condition of temperature and pressure (Fig. 1). The apparatus will be described in detail later. The dry core was initially evacuated and then saturated with ZnO/SiO<sub>2</sub> nanofluid. For this purpose, three to four pore volumes (PV) of nanofluid was injected at a fixed flow rate of 2 cc/min. The nanofluid-saturated core was

then aged in the nanofluid at 80 °C and 3000 psig for 48 h. After that, nearly 5 PVs of brine was injected to displace the nanofluid and wash the

core, followed by evacuation for about 6 h. At last, the core was removed from its holder and dried in an oven at 80 °C.



Fig. 1. Experimental set up for core displacement tests and chemical treatment.

## 2.4. Characterization

Fourier transform infrared spectroscopy (FTIR) spectra were acquired on a Bruker tensor 27 spectrometer to evaluate the functional groups of the synthesized nanocomposites in the wavenumber range of 4000–400  $\text{cm}^{-1}$ . The surface morphology of ZnO/SiO<sub>2</sub> nanocomposites and the carbonate core with and without wettability alteration were revealed by scanning electron microscope (SEM) (KYKY model EM3200). X-ray diffraction (XRD) was used to study the size and crystallinity of the nanocomposites using Bruker D8-Advance diffractometer with Cu K $\alpha$  radiation ( $\lambda=1.54\text{\AA}$ ). The surface topography and roughness of the treated and untreated core sample were determined by stylus profilometer (SP) (Dektak XT from Bruker). Energy dispersive X-ray (EDX) (SiriusSD) was used to characterize the surface elemental composition of the carbonate core before and after treatment with nanofluid.

## 2.5. Contact angle measurement

To study the wettability of the core quantitatively and evaluate preliminary the superamphiphobicity of nanofluid, the gas–liquid–rock contact angle was measured using an in-house contact angle measurement device (Fig. 2a). The static contact angles of aqueous and oil phases as probe liquids in air medium and at room temperature were measured using sessile drop technique. In each measurement, a  $\sim 5\ \mu\text{l}$  drop of liquid was released from an accurate syringe on the surface of the core sample. A CCD camera with the microscopic lens was used to visualize the process and taking side images of high-resolution magnified liquid droplet, under sufficient illumination of the light source. Each contact angle measurement was repeated for 3–5 times at different locations on the solid surface and the average value was reported. Dynamic contact angles were also measured by force tensiometer KSV Sigma 700, using the Wilhelmy method (Fig. 2b).

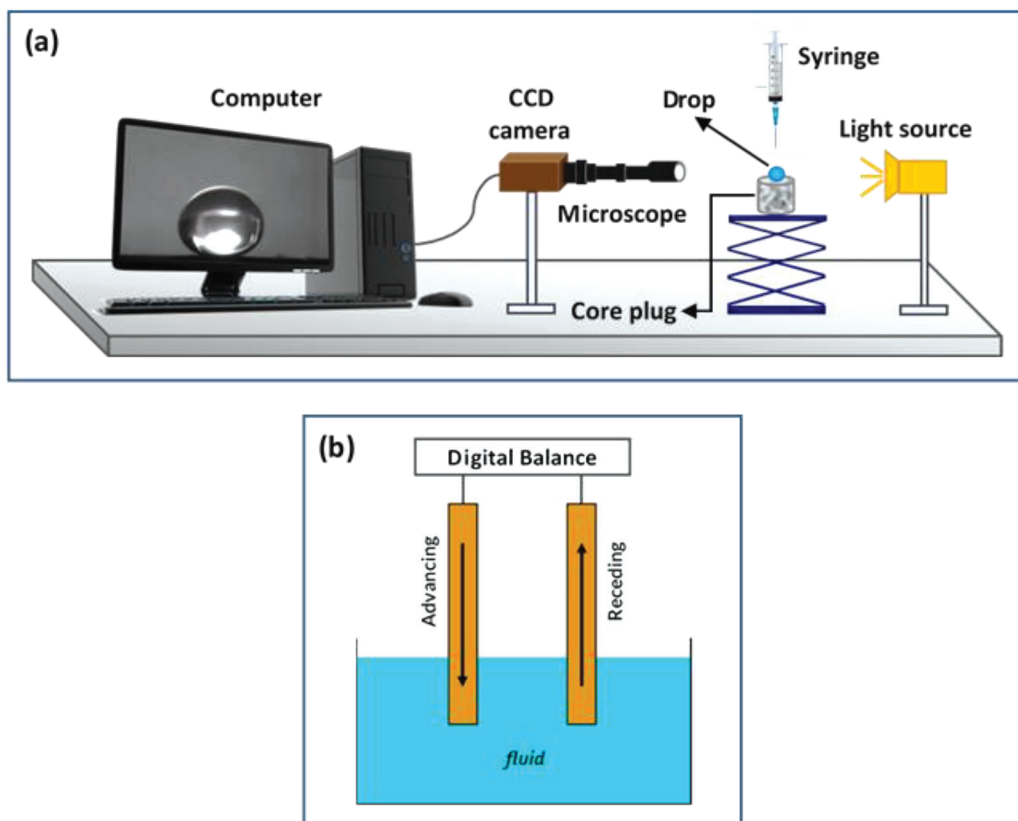


Fig. 2. Schematic for (a) static and (b) dynamic contact angle measurements.

## 2.6. Coreflooding apparatus and test procedure

Fluid flow tests were performed in core scale to investigate the efficiency of ZnO/SiO<sub>2</sub> nanofluid in wettability alteration to gas-wetting under reservoir temperature and pressure conditions. Fig. 3 illustrates a schematic of the coreflooding setup for the unsteady-state gas/liquid flow with gas displaced by liquid injection. The coreflooding apparatus contains high-pressure displacement pumps (Schlumberger DBR) with process control system for injecting the fluid at constant rate, a back pressure regulator for controlling the downstream core pressure, a differential pressure transducer (Rosemount 3051) for measuring the pressure drop across the core and a data acquisition system for collecting and storing the differential pressure information. The gas and liquid are discharged through the back pressure regulator and transmitted to a separator. The effluent Liquid is collected in a calibrated tube and the amount of it measured

versus time. The outlet gas flow rate is also measured by a mass flow meter (Alicat M) in the range of 0-50 cm<sup>3</sup>/s with the accuracy of about 0.8%. Other apparatuses such as liquid transfer vessels and a cylindrical core holder were placed inside a temperature-controlled oven. The core sample is fixed inside the core holder covered with a Viton rubber sleeve to confine the core. The core holder is placed horizontally to avoid gravity effect. For packing the core, an overburden pressure of 800-1000 psig above the inlet pressure is applied. The temperature of the system was maintained at 80 °C during all tests, which is high enough for most reservoir applications.

The goal of this study is to quantify the effectiveness of the nanofluid by measuring the effective and relative permeability of liquid flow in gas/oil or gas/water systems through liquid flooding of a gas-saturated core. Before wettability alteration, the core was evacuated first by a vacuum pump to get rid of air and

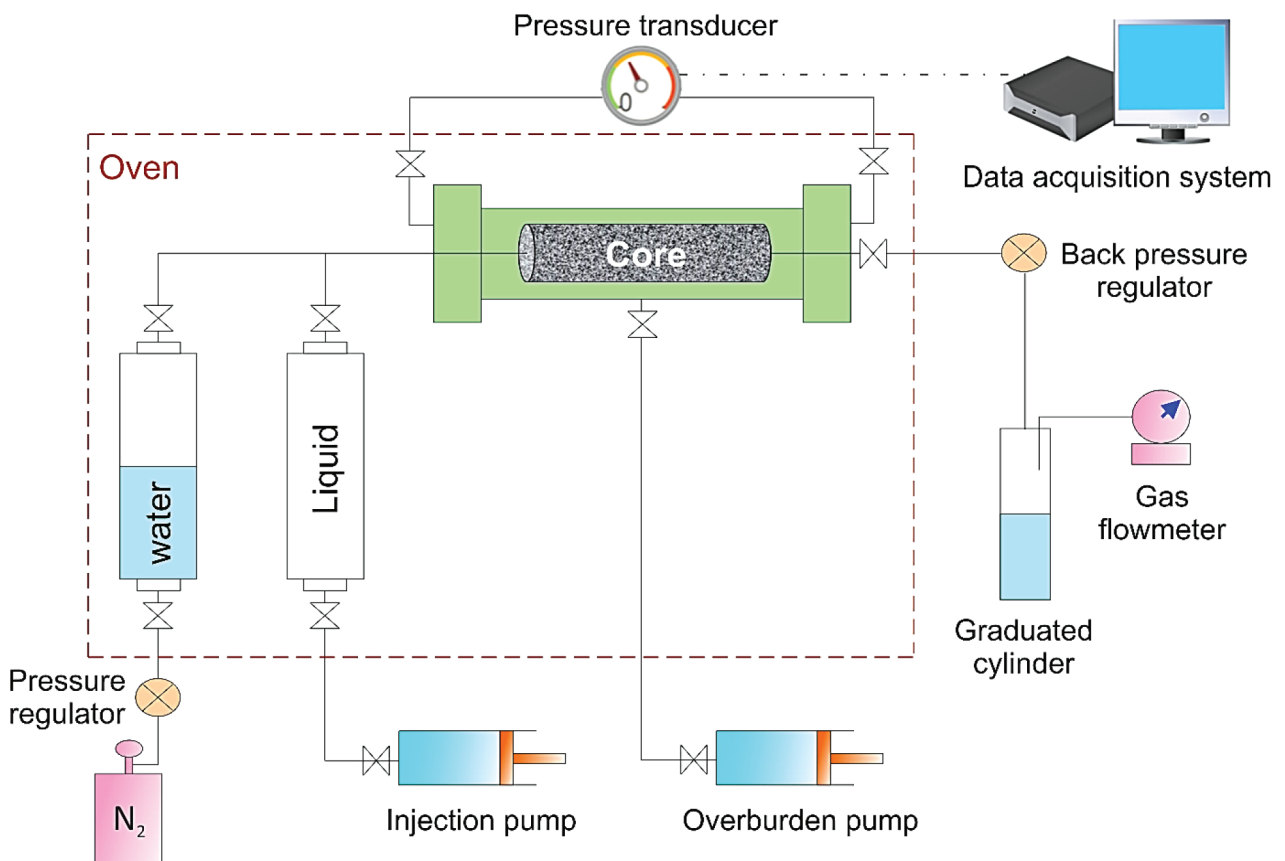


Fig. 3. Schematic of apparatus for core flooding experiments.

then it was saturated with the nitrogen which injected at a constant injection pressure by a gas-pressure regulator. Next, the displacement process of gas was started by injection of liquid (brine or gas-condensate) at a constant rate. The amount of produced gas and liquid versus time was recorded until surely no more gas recovered. Moreover, the transient pressure drop is recorded until steady-state is obtained. The effective and relative permeability of liquid flow were calculated subsequently, as explained in section 3.3. After that, the core was cleaned by a solvent and dried and evacuated before starting the next test.

After conducting the evaluation testing in the untreated core, the wettability alteration tests. Were performed for this purpose, the core was treated with nanofluid (as described earlier in section 2.3.2.) and the same experiments to those performed for untreated core were repeated to calculate the effective and relative permeability of the liquid flow after the wettability alteration.

### 3. Results and Discussion

#### 3.1. Characterization of ZnO/SiO<sub>2</sub> nanocomposites

To confirm the formation of ZnO/SiO<sub>2</sub> through the synthesis process, the FTIR spectrum of the ZnO/SiO<sub>2</sub> nanocomposites is shown in Fig. 4. The bands positioned at 459, 577 and 615 cm<sup>-1</sup> are attributed to Zn–O stretches [32,33]. The peaks at 868 cm<sup>-1</sup> are related to the Si–O–Si asymmetric stretching vibrations while the peak at 979 cm<sup>-1</sup> is for the Si–O–Si symmetric stretching [34]. The peak observed at 1457 cm<sup>-1</sup> corresponds to Si–OH stretching vibration [34]. Furthermore, peak at 1628 cm<sup>-1</sup> and a broad band at 3445 cm<sup>-1</sup> are associated with O–H bending and O–H stretching vibrations of ZnO/SiO<sub>2</sub> [34]. Moreover, the appearance of the absorption band at 933 cm<sup>-1</sup> is assigned to the Si–O–Zn stretching which confirms that SiO<sub>2</sub> indeed binds with ZnO [35].

The SEM image for the synthesized nanocomposites is presented in Fig. 5. It can be seen that the ZnO/SiO<sub>2</sub> nanostructures consist of the hybrid morphologies of nanospheres and nanoplates.

Fig. 6 illustrates the XRD patterns for the as-prepared ZnO/SiO<sub>2</sub> nanocomposites. The measured diffraction angles are reasonably compatible with the standard spectrum of willemite Zn<sub>2</sub>SiO<sub>4</sub> (JCPDS card number 37–1485), indicating that the crystallographic structure of these nanocomposites is hexagonal. The diffraction peaks at  $2\theta=31.48^\circ, 33.95^\circ, 36.18^\circ, 65.58^\circ, 55.92^\circ, 48.89^\circ$  and  $66.68^\circ$  can be attributed to the (100), (002), (101), (102), (110), (112) and (201) planes of ZnO, respectively [36,37]. The average crystallite size of ZnO/SiO<sub>2</sub> nanocomposites are calculated from the XRD analysis and Sherrer's equation,

$$t = \frac{0.9\lambda}{\beta \cos\theta} \quad (1)$$

where  $t$  is the full-width-at-half-maximum (fwhm) of the diffracted peak,  $\theta$  is the diffraction angle, and  $\lambda$  is the wavelength of X-ray radiation (1.548 Å for Cu K $\alpha$ ). The estimated average crystallite size value for ZnO/SiO<sub>2</sub> nanocomposites is found to be 46 nm.

#### 3.2. Contact angle determination and surface characterization

The wetting properties of carbonate core rock without and with wettability alteration to gas-wetting by nanofluid were identified through contact angle measurements of distilled water and 2 wt% NaCl brine as the aqueous phase, and n-decane and gas-condensate as the oil phases. The native carbonate plate was completely wetted by both water and oil liquid drops, which indicates the fact that the carbonate sample is strongly liquid-wet (i.e., the static contact angle of water and oil = 0°). However, the measured distilled water, brine, n-decane, and condensate contact angles of the rock plate were exceeded to 162°, 162°, 136°, and 135°, respectively, after treatment with nanofluid which demonstrates the superhydrophobic property of the treated surfaces. According to this results, ZnO/SiO<sub>2</sub> nanofluid has successfully increased the contact angle of water and oil drops to a much greater degree than the various chemicals reported in the previous studies [5-14,28,29]. Fig. 7 shows the brine and condensate contact angles on the surface of a rock plate, before and after wettability alteration.

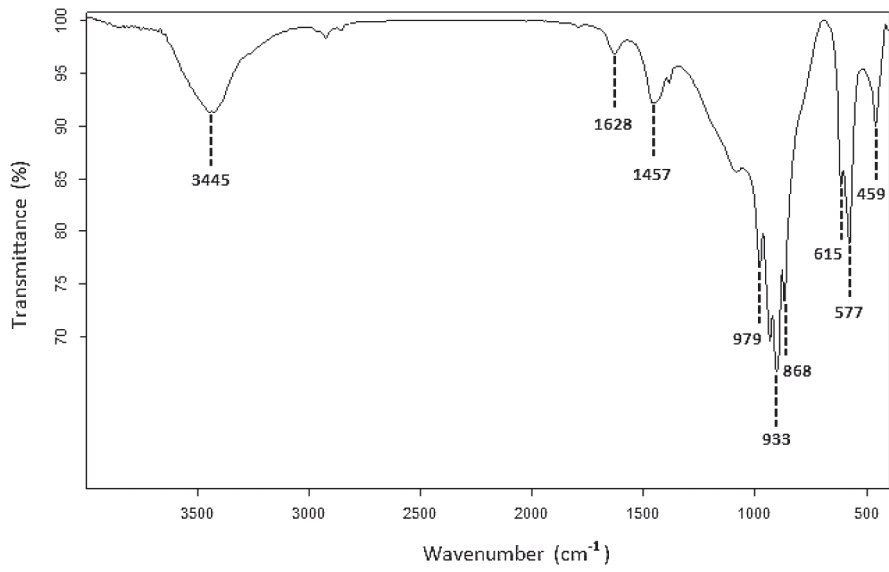


Fig. 4. FTIR spectra of ZnO/SiO<sub>2</sub> nanocomposite powders in 4000–400 cm<sup>-1</sup> region.



Fig. 5. SEM image of synthesized ZnO/SiO<sub>2</sub> nanocomposites.

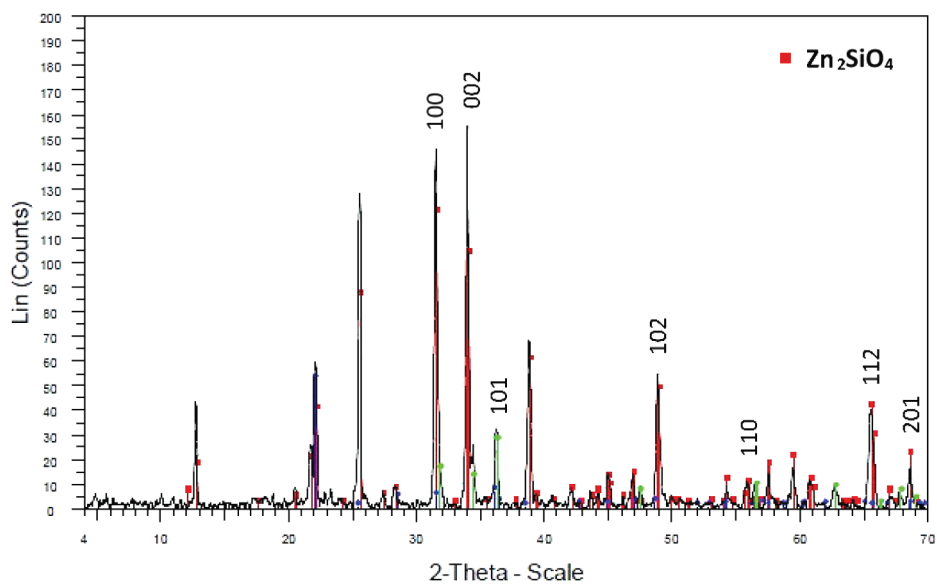


Fig. 6. XRD pattern of hexagonal ZnO/SiO<sub>2</sub> nanostructures.

Furthermore, it was observed that the aqueous phase droplets freely rolled-off on the treated core surface while there was no apparent tilt of the surface ( $2^\circ$ ), which made it difficult to control for measuring the static contact angle. Such a minimum sliding angle reveals that water has low adhesion to the rock surface and the core sample gained self-cleaning property [38,39]. Besides, it is known that for the self-cleaning property of a liquid-repellent surface, contact angle hysteresis of  $10^\circ$  is desired [40,41]. Contact angle hysteresis which is defined as the difference between the advancing and receding angles was measured using the Wilhelmy method. The value of contact angle hysteresis for the rock plate treated with nanofluid was measured quasi-null for the aqueous phase. Such an ultralow contact angle hysteresis, confirms that the rock surface benefits the drop-rolling ability and the self-cleaning property as well.

The improved hydrophobicity, oleophobicity, and self-cleaning properties of the treated rock are attributed to the combination of surface roughening by the ZnO/SiO<sub>2</sub> nanocomposites and lowering the surface energy by fluoro-containing coating [42-44]. The surface topography is generally known as the decisive factor in specifying the liquid-repellency of rough surfaces. Therefore, SP analysis and SEM images were employed to study the morphological features of the core surface structure. Fig. 8 illustrates the SP micrographs of both native rock plate and treated rock plate with nanofluid. Fig. 8a indicates that the pristine rock substrate generally offers a primary roughness with microscale structure. Regarding the corresponding contact angles of water and oil drops which are equal to  $0^\circ$ , the liquid-wetting nature of native rock plate can be ascribed to the several cavities existed throughout the roughness, which allows the liquids entering easily into them. After treatment, the deposition of nanofluid's contents provides the secondary roughness to repel the liquid penetration, referring the Cassie model [45]. In other words, the hierarchial rough structure on the surface, similar to the structure of a lotus leaf [44], can simply trap a large amount of microscopic air

layer in the craters between the protrusions that reduces the contact area between the liquid and the surface. The air pocket makes a floating force against water and oil drops that leads to superamphiphobicity.

Besides the surface roughening by ZnO/SiO<sub>2</sub> nanocomposites, using the fluoro-containing materials as PTFE, TFE and PFOS solution enhanced the liquid-repellency of the core surface, especially the oleophobicity, owing to impressive reduction of surface free energy. TFE and PFOS have very low surface energy owing to their high content of  $-CF_3$  and  $-CF_2$  groups.  $-CF_3$  terminated surfaces are known to possess the lowest surface free energy of  $\sim 6 \text{ mN m}^{-1}$  followed by  $-CF_2$  groups as the next lowest [46-48]. Teflon also has the low surface energy of  $18.5 \text{ mN m}^{-1}$  [48]. Hence, the deposition of fluorochemicals on the outermost layer of surface coating decreases the surface energy and the intrusion of liquids into cavities of the surface.

SEM investigations of the carbonate plate before and after wettability alteration to gas-wetting, distinctly confirm the formation of a layer containing fluorochemicals and ZnO/SiO<sub>2</sub> nanocomposites on the microstructure core surface, after treatment with nanofluid (Fig. 9). The average size of the sphere-like nanotextures was determined to be in the range of 34-60 nm in diameter.

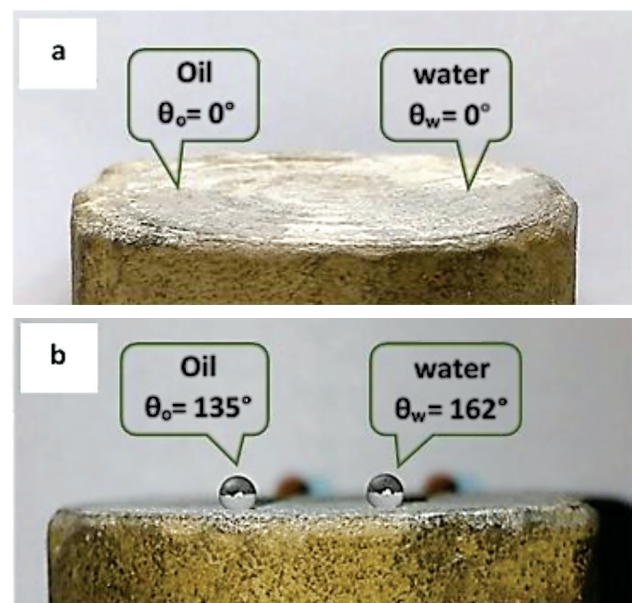


Fig. 7. Static Contact angle of brine and gas-condensate on the surface of carbonate rock plate (a) before and (b) after wettability alteration.

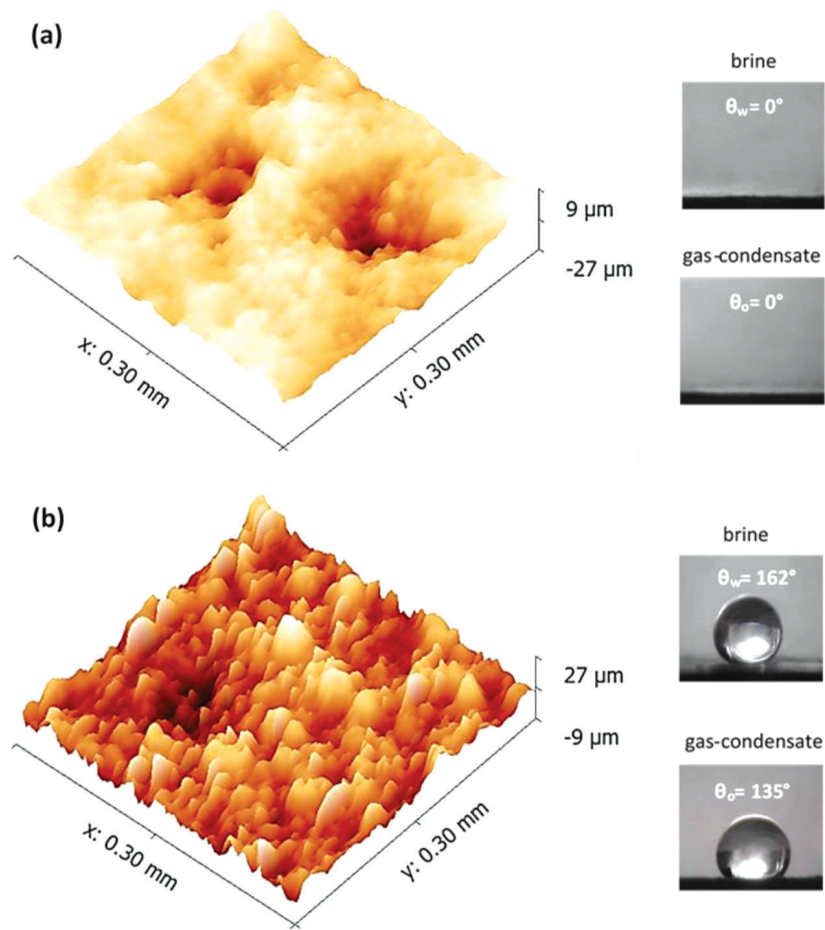


Fig. 8. 0.3 mm × 0.3 mm 3D SP topography images of the (a) untreated and (b) treated core substrate. Cross-view shapes of brine and gas-condensate droplets placed on the corresponding surfaces are shown in the insets.

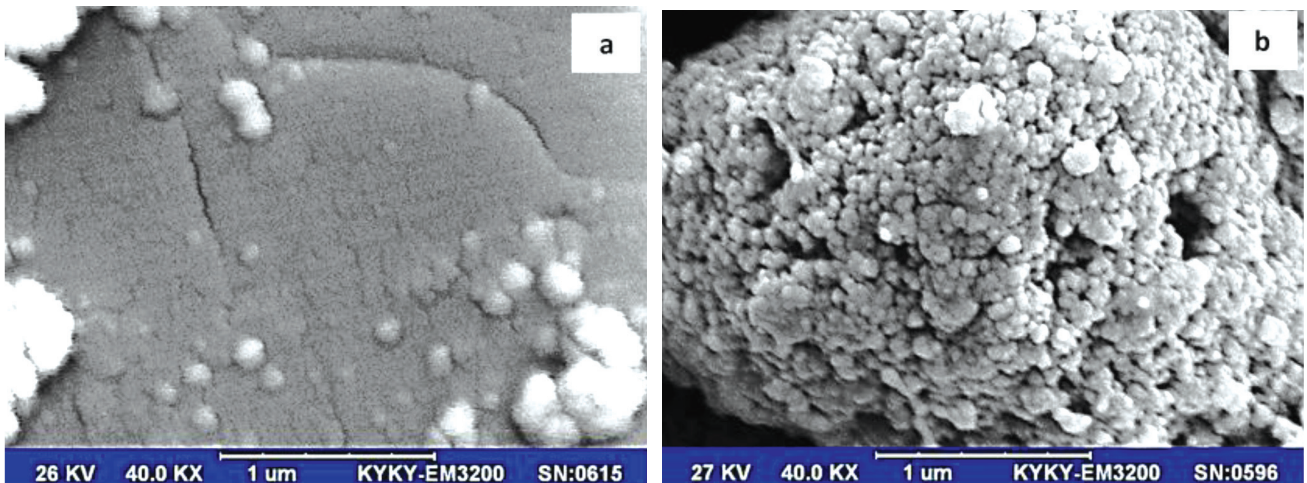


Fig. 9. SEM images of (a) untreated rock plate and (b) treated rock plate with ZnO/SiO<sub>2</sub> nanofluid.

### 3.3. Core displacement results

After a preliminary evaluation of the formulated nanofluid by contact angle

measurements, fluid flow tests were used to investigate the effect of wettability alteration on water and condensate blocking in the

carbonate core. The result of pressure drop across the core as a function of pore volumes injected of liquid is presented in Fig. 10. As seen from Fig. 10a for gas/water system, in both untreated and treated cores, the pressure drop increases initially until it reaches the maximum value. Afterward, the pressure drop decreases gradually and stabilized at a constant value of 15.0 psi for untreated core and 6.5 psi for treated core at the steady-state. Hence, nanofluid treatment reduced the steady-state two-phase flow pressure drop about 56%. The same trend is also observed in gas/oil system (Fig. 10b), with the pressure drop plateaus at 17.7 psi for untreated core and 7.8 psi for treated core. The treatment of carbonate core with nanofluid could also improve the steady-state pressure drop of this case about 56%. These results imply the pronounced capability of the nanofluid in altering the wettability from liquid-wetting (hydrophilic and oleophilic) to ultra gas wetting (superamphiphobic).

The single-phase liquid-injection in a core saturated with gas is a transient two-phase gas/liquid flow experiment in which the gas inside the core is displaced by the liquid. In late stage of liquid injection, when the residual gas is left in the core and the pressure drop reaches steady-state, we apply Darcy's law for calculating the effective permeability of liquid flow ( $K_{el}$ ):

$$\Delta p = Q_l \left( \frac{\mu_l}{K_{el}} \right) \left( \frac{L}{A} \right) \quad (2)$$

where the pressure ( $\Delta p$ ) is described as a function of the liquid volumetric flow rate ( $Q_l$ ), with the parameters of core length ( $L$ ), Liquid viscosity ( $\mu_l$ ), cross-sectional area ( $A$ ), and the liquid effective permeability ( $K_{el}$ ).

The liquid relative permeability ( $K_{rl}$ ) is also calculated from the ratio of the liquid effective permeability to the liquid absolute permeability ( $K_l$ ) which is received from single-phase liquid flow:

$$K_{rl} = \frac{K_{el}}{K_l} \quad (3)$$

The absolute permeability to water was measured to be 11 and 10.4 mD for untreated and treated core, respectively, which demonstrates the treatment of the core with nanofluid slightly reduces the absolute permeability due

to plugging of small pore throats.

We quantify the nanofluid treatment effectiveness in liquid flow then by calculating the change in the liquid effective and relative permeability as follows:

$$\frac{\Delta K_{el}}{K_{el}} \equiv \frac{K_{el}(\text{treated core}) - K_{el}(\text{untreated core})}{K_{el}(\text{untreated core})} \quad (4)$$

$$\frac{\Delta K_{rl}}{K_{rl}} \equiv \frac{K_{rl}(\text{treated core}) - K_{rl}(\text{untreated core})}{K_{rl}(\text{untreated core})} \quad (5)$$

Table 1 gives the results of calculated effective and relative permeability of liquid flow in the pre-treated and post-treated cores. It is obvious, the treatment of core with ZnO/SiO<sub>2</sub> nanofluid predominantly increases the brine and gas-condensate mobility under reservoir condition, according to increase in the effective and relative permeability of liquid. The results support the theory that the nanofluid successfully alters the wettability of carbonate core from strongly liquid-wetting to the ultra gas-wetting condition.

In order to investigate the penetration of the nanocomposites and fluorine species into the pores of carbonate core, since the coreflooding tests were accomplished, we have cut the core by a trimming machine from middle along the radius and analyzed the surface chemical composition by EDX spectra. As evidence from Fig. 11, the surface of native carbonate core is mainly composed of Ca, C and O elements. After treatment with nanofluid, the constituent materials of ZnO/SiO<sub>2</sub> nanofluid containing of Si and Zn elements as nanocomposite, and F element which comes from fluorochemicals were determined on the surface. The presence of these elements reflect the ability of nanocomposites accompanied with fluorochemicals to diffuse into the core and adsorb onto the surface.

Moreover, it is noteworthy to point out that the quality of the contact angle of brine and condensate drops on the treated rock plate in small slab scale and core scale (after injection of 5 PVs of water to displace the nanofluid) demonstrates the durability of nanofluid treatment at the reservoir conditions.

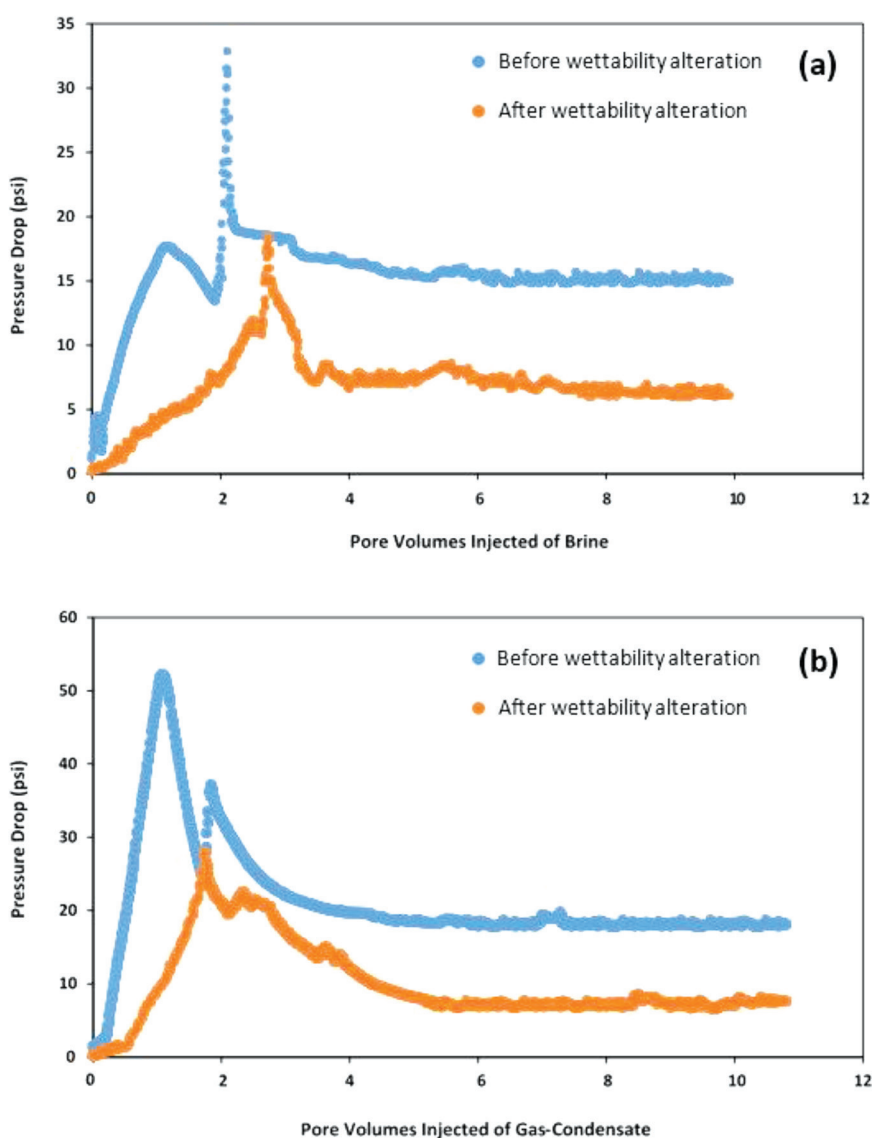


Fig. 10. The pressure drop across the core versus pore volumes injected of (a) brine and (b) condensate before and after treatment with ZnO/SiO<sub>2</sub> nanofluid.

Table 1. Liquid effective permeability and relative permeability data, before and after wettability alteration

System	Liquid effective and relative permeability					
	Pre-treatment		Post-treatment		change	
	$K_{el}$ (mD)	$K_{rl}$	$K_{el}$ (mD)	$K_{rl}$	(%) $\Delta K_{el} / K_{el}$	(%) $K_{rl} / K_{rl}$
Gas/Brine	3.20	0.29	7.38	0.70	+130	+141
Gas/liquid condensate	3.60	0.33	8.14	0.78	+126	+136

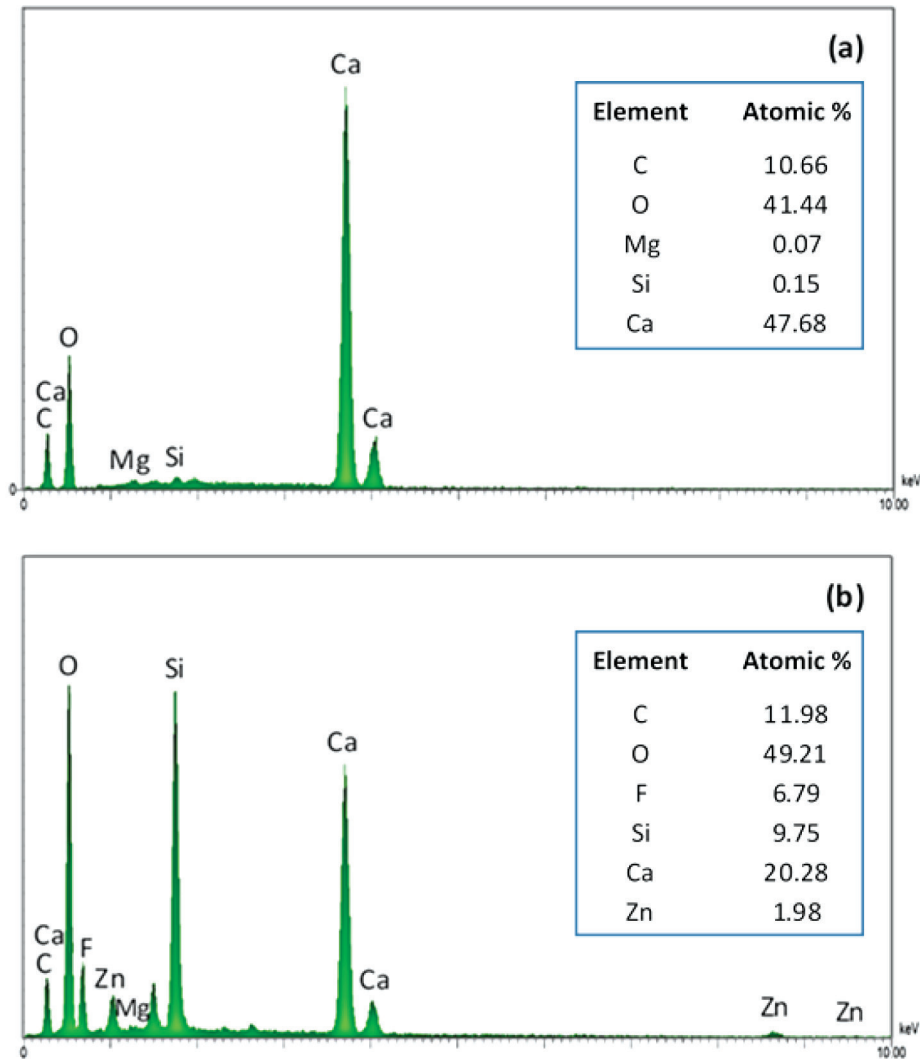


Fig. 11. EDX analysis of carbonate core (a) before and (b) after aging in ZnO/SiO<sub>2</sub> nanofluid.

#### 4. Conclusion

Liquid blockage (water or condensate accumulation) near the wellbore regions leads to major productivity reduction in gas condensate reservoirs. Through wettability alteration to gas-wetting, the mobility of liquid phase for a gas/liquid system increases remarkably, showing great potential for enhancing the gas-well deliverability. It is successfully changed the wettability of carbonate reservoir rocks from strongly liquid-wetting to super water- and highly oil-repellent condition using a novel formulated nanofluid consisted of synthesized ZnO/SiO<sub>2</sub> nanocomposites and fluorochemicals PTFE, TFE, and PFOS. The water

(distilled water or brine) and oil (n-decane or liquid gas-condensate) contact angle increased significantly from 0° to 162° and about 135°, respectively, after treatment of the rock with the prepared nanofluid. It is also observed that the rock surface exhibit excellent self-cleaning ability due to the minimum contact angle hysteresis (0°) and very low sliding angle (<2°) for water. Surface characterization of the treated plates was carried out by SEM, SP, and EDX analyses. Accordingly, the improved super liquid-repellency is attributed to the roughness of the nanocomposites that adsorb onto microscale texture of rock and the low surface energy of fluoro-containing materials. Moreover, our measurements of core displacement tests indicate that treatment of wettability

alteration to ultra gas-wetting using ZnO/SiO<sub>2</sub> nanofluid is promisingly effective. It is found that such a wettability alteration decreases the pressure drop across the core which leads to a reduction of the amount of liquid trapping in pore space owing to a dominant increase in the liquid relative permeability. It is supposed the achieved results would pave the way for solving the problem of condensate blockage in gas condensate reservoirs.

## Acknowledgments

The authors sincerely wish to thank Dr. Matthias Menzel from Fraunhofer Institute for Microstructure of Materials and Systems IMWS, Halle (Germany) for performing SP experiments. We do also gratefully acknowledge Dr. Pegah Esmailzadeh and Dr. Stefan L. Schweizer from Martin Luther University Halle-Wittenberg of Germany for their worthful help with the SP analyses.

## References

- [1] D. Afidick, N.J. Kaczorowski, S. Bette, Production performance of a retrograde gas reservoir: a case study of the Arun Field, in: SPE Asia Pacific Oil and Gas Conference, Melbourne, Australia, 1994.
- [2] A. El-Banbi, W.D. McCain, M.E. Semmelbeck, Investigation of well productivity in gas-condensate reservoirs, in: SPE/CERI Gas Technology Symposium, Calgary, Canada, 2000.
- [3] M.P. Cimolai, R.M. Gies, D.B. Bennion, D.L. Myers, Mitigating horizontal well formation damage in a low-permeability conglomerate gas reservoir, in: SPE gas Technology Symposium, Calgary, Canada, 1993.
- [4] K. Li, A. Firoozabadi, Phenomenological modeling of critical condensate saturation and relative permeabilities in gas/condensate systems, SPE Journal, 5 (2000) 138-147.
- [5] K. Li, A. Firoozabadi, Experimental study of wettability alteration to preferential gas-wetting in porous media and its effects, SPE Reservoir Evaluation and Engineering, 3 (2000) 139-149.
- [6] G.Q. Tang, A. Firoozabadi, Wettability alteration to intermediate gas-wetting in porous media at elevated temperatures, Transport in Porous Media, 52 (2003) 185-211.
- [7] V. Kumar, G.A. Pope, M.M. Sharma, Improving the gas and condensate relative permeability using chemical treatment, in: SPE Gas Technology Symposium, Calgary, Canada, 2006.
- [8] M. Fahes, A. Firoozabadi, Wettability alteration to intermediate gas-wetting in gas condensate reservoirs at high temperatures, SPE Journal, 12 (2007) 397-407.
- [9] M. Noh, A. Firoozabadi, Wettability alteration in gas-condensate reservoirs to mitigate well deliverability loss by water blocking, SPE Reservoir Evaluation and Engineering, 11 (2008) 676-685.
- [10] X. Xie, Y. Liu, M. Sharma, W.W. Weiss, Wettability alteration to increase deliverability of gas production wells, Journal of Natural Gas Science and Engineering, 1 (2009) 39-45.
- [11] S. Wu, A. Firoozabadi, Permanent Alteration of porous media wettability from liquid-Wetting to intermediate gas-wetting, Transport in Porous Media, 85 (2010) 189-213.
- [12] K. Li, Y. Liu, H. Zheng, G. Huang, G. Li, Enhanced gas-condensate production by wettability alteration to gas wetness, Journal of Petroleum Science and Engineering, 78 (2011) 505-509.
- [13] S. Sharifzadeh, S. Hassanajili, M.R. Rahimpour, Wettability alteration of gas condensate reservoir rocks to gas wetness by sol-gel process using fluoroalkylsilane, Journal of Applied Polymer Science, 128 (2012) 4077-4085.
- [14] C. Feng, Y. Kong, G. Jiang, J. Yang, C. Pu, Y. Zhang, Wettability modification of rock cores by fluorinated copolymer emulsion for the enhancement of gas and oil recovery, Applied Surface Science, 258 (2012) 7075-7081.
- [15] S.K. Das, S.U.S. Choi, W. Yu, T. Pradeep, Nanofluids: Science and Technology, John Wiley & Sons, Inc Publishing, Hoboken, New Jersey, 2008.
- [16] R. Taylor, S. Coulombe, T. Otanicar, P. Phelan, A. Gunawan, W. Lv, G. Rosengarten, R. Prasher, H. Tyagi, Small particles, big impacts: a review of the diverse applications of nanofluids, Journal of Applied Physics, 113 (2013) 0113011-01130119.
- [17] D. Tripathi, O. Bég, A study on peristaltic flow of nanofluids: Application in drug delivery systems, International Journal of Heat and Mass Transfer, 70 (2014) 61-70.
- [18] H.T. Phan, N. Caney, P. Marty, S. Colasson, J. Gavillet, Surface coating with nanofluids: the effect of pool boiling heat transfer, Nanoscale and Microscale Thermo Physical Engineering, 14 (2010) 229-244.
- [19] D. Wen, G. Lin, S. Vafaei, K. Zhang, Review of nanofluids for heat transfer applications, Particuology, 7 (2009) 141-150.
- [20] D.T. Wasan, A.D. Nikolov, Spreading of nanofluids on solids, Nature, 423 (2003) 156-159.

- [21] R. Saidur, K.Y. Leong, H.A. Mohammad, A review on applications and challenges of nanofluids, *Renewable and Sustainable Energy Reviews*, 15 (2011) 1646-1668.
- [22] A. Karimi, Z. Fakhroueian, A. Bahramian, N. Pour Kh-iabani, J. Babaei Darabad, R. Azin, S. Arya, Wettability Alteration in Carbonates using Zirconium Oxide Nanofluids: EOR Implications, *Energy and Fuels*, 26 (2012) 1028-1036.
- [23] L. Hendraningrat, O. Torsæter, A coreflood investigation of nanofluid enhanced oil recovery, *Journal of Petroleum Science and Engineering*, 111 (2013) 128-138.
- [24] B.A. Suleimanov, F.S. Ismailov, E.F. Veliyev, Nanofluid for enhanced oil recovery, *Journal of Petroleum Science and Engineering*, 78 (2011) 431-437.
- [25] J.S. Nam, P. Lee, S.W. Lee, Experimental characterization of micro-drilling process using nanofluid minimum quantity lubrication, *International Journal of Machine Tools and Manufacture*, 51 (2011) 649-652.
- [26] S. Mokhatab, M.A. Fresky, M.R. Islam Applications of nanotechnology in oil and gas E&P, *Journal of Petroleum Technology*, 58 (2006) 48-51.
- [27] M.S. Zaman, M.R. Islam, S. Mokhatab, Nanotechnology Prospects in the Petroleum Industry, *Petroleum Science and Technology*, 30 (2012) 1053-1058.
- [28] M. Mousavi, S. Hassanajili, M.R. Rahimpour, Synthesis of fluorinated nano-silica and its application in wettability alteration near-wellbore region in gas condensate reservoirs, *Applied Surface Science*, 273 (2013) 205-214.
- [29] M. Aminnaji, H. Fazeli, A. Bahramian, S. Gerami, H. Ghojavand, Wettability alteration of reservoir rocks from liquid wetting to gas wetting using nanofluid, *Transport in Porous Media*, 109 (2015) 201-206.
- [30] Y. Hwang, J. Lee, J. Lee, Y. Jeong, S. Cheong, Y. Ahn, S. Kim, Production and dispersion stability of nanoparticles in nanofluids, *Powder Technology*, 186 (2008) 145-153.
- [31] A. Ghadimi, R. Saidur, M. H., A review of nanofluid stability properties and characterization in stationary conditions, *International Journal of Heat and Mass Transfer*, 54 (2011) 4051-4068.
- [32] I. Uysal, F. Severcana, Z. Evis, Characterization by Fourier transform infrared spectroscopy of hydroxyapatite co-doped with zinc and fluoride, *Ceramics International*, 39 (2013) 7727-7733.
- [33] K. Sowri babu, A. ramachandra Reddy, C. Sujatha, K. Venugopal Reddy, A.N. Mallika, Synthesis and optical characterization of porous ZnO, *Journal of Advanced Ceramics*, 2 (2013) 260-265.
- [34] J.V.G. Tinio, K.T. Simfroso, A.D.M. Peguit, R.T. Candidato Jr, Influence of OH<sup>-</sup> Ion Concentration on the Surface Morphology of ZnO-SiO<sub>2</sub> Nanostructure, *Journal of Nanotechnology*, 2015 (2015) 1-7.
- [35] E.G. Pantohan, R.T. Candidato Jr, R.M. Vequizo, Surface characteristics and structural properties of sol-gel prepared ZnO-SiO<sub>2</sub> nanocomposite powders, *IOP Conference Series: Materials Science and Engineering*, 79 (2015) 1-6.
- [36] J. El Ghoul, K. Omri, L. El Mir, C. Barthou, S. Alaya, Sol-gel synthesis and luminescent properties of SiO<sub>2</sub>/Zn<sub>2</sub>SiO<sub>4</sub> and SiO<sub>2</sub>/Zn<sub>2</sub>SiO<sub>4</sub>:V composite materials, *Journal of Luminescence*, 132 (2012) 2288-2292.
- [37] S. Tripathi, R. Bose, R. Roy, S. Nair, N. Ravishankar, Synthesis of hollow nanotubes of Zn<sub>2</sub>SiO<sub>4</sub> or SiO<sub>2</sub>: mechanistic understanding and uranium adsorption behavior, *Applied Materials and Interfaces*, 7 (2015) 26430-26436.
- [38] H. Butt, C. Semprebon, P. Papadopoulos, D. Vollmer, M. Brinkmann, M. Ciccotti, Design principles for superamphiphobic surfaces, *Soft Matter*, 9 (2013) 418-428.
- [39] N. Valipour Motlagh, F.C. Birjandi, J. Sargolzaei, N. Shahtahmassebi, Durable, superhydrophobic, superoleophobic and corrosion resistant coating on the stainless steel surface using a scalable method, *Applied Surface Science*, 283 (2013) 636-647.
- [40] H. Ogihara, J. Xie, J. Okagaki, T. Saji Simple Method for Preparing Superhydrophobic Paper: Spray-Deposited Hydrophobic Silica Nanoparticle Coatings Exhibit High Water-Repellency and Transparency, *Langmuir* 28 (2012) 4605-4608.
- [41] P. Muthiah, B. Bhushan, K. Yun, H. Kondo, Dual-layered-coated mechanically-durable superomniphobic surfaces with anti-smudge properties, *Journal of Colloid and Interface Science*, 409 (2013) 227-236.
- [42] M. Nosonovsky, B. Bhushan, Superhydrophobic surfaces and emerging applications: Non-adhesion, energy, green engineering, *Current Opinion in Colloid and Interface Science*, 14 (2009) 270-280.
- [43] E. Celia, T. Darmanin, E.T. Givenchy, S. Amigoni, F. Guittard, Recent advances in designing superhydrophobic surfaces, *Journal of Colloid and Interface Science*, 402 (2013) 1-18.
- [44] N. Valipour Motlagh, F.C. Birjandi, J. Sargolzaei, Super-non-wettable surfaces: A review, *Colloids and Surfaces A: Physicochemical and Engineering Aspects*, 448 (2014) 93-106.
- [45] A.B.D. Cassie, S. Baxter, Wettability of porous surfaces, *Transactions of the Faraday Society*, 40 (1994) 546-551.
- [46] Q. Xie, J. Xu, L. Feng, L. Jiang, W. Tang, X. Luo, C.C. Han, Facile creation of a super-amphiphobic coating surface with bionic microstructure, *Advanced Materials*, 16 (2004) 302-305.
- [47] T. Nishino, M. Meguro, K. Nakamae, M. Matsushita, Y. Ueda, The lowest surface free energy based on -CF<sub>3</sub> alignment, *Langmuir*, 15 (1999) 4321-4323.
- [48] S. Shibuichi, T. Yamamoto, T. Onda, K. Tsujii, Super water- and Oil-repellent surfaces resulting from fractal structure, *Journal of Colloid and Interface Science*, 208 (1998) 287-294.

## تغییر ترشوندگی سنگ مخازن گاز میعانی در نواحی نزدیک به چاه به منظور کاهش انسداد مایع، از طریق پوشش دهی سنگ با نانوسیال دارای خاصیت ابر آبگریزی و ابر نفت گریزی ساخته شده بر پایه ی نانوکامپوزیت $ZnO/SiO_2$

• پوریا اسماعیل زاده، محمدتقی صادقی

• دانشگاه علم و صنعت ایران، دانشکده مهندسی شیمی، تهران، ایران

• علیرضا بهرامیان

• دانشگاه تهران، انستیتو مهندسی نفت، تهران، ایران

### چکیده

در مخازن گاز میعانی بر اثر کاهش فشار مخزن به زیر فشار نقطه‌ی شبنم هیدروکربوری سیال مخزن، میعانات گازی از فاز گاز جدا شده، به فاز مایع منتقل می‌شود و در نواحی اطراف چاه تجمع می‌یابند. در صورت بروز این پدیده که به انسداد میعانی مرسوم است نفوذپذیری نسبی فاز گاز و در نتیجه نرخ تولید گاز از چاه به شدت کاهش می‌یابد. یکی از روش‌هایی که پتانسیل قابل توجهی برای رفع این پدیده و افزایش بهره‌دهی چاه در اختیار دارد تغییر ترشوندگی سنگ مخازن گاز میعانی از حالت مایع دوست به گاز دوست می‌باشد. در این مقاله، از نانوسیالی حاوی نانوکامپوزیت سنتز شده ی  $ZnO/SiO_2$  و مواد فلئوردار PTFE، PFOS، TFE و برای تغییر ترشوندگی سنگ کربناته‌ی مخزن گاز میعانی از حالت شدیداً مایع دوست به حالت ابر آبگریز و ابر نفت گریز توأم (ابر گاز دوست) استفاده شد. بطوریکه زاویه تماس آب نمک و نمونه میعانات گازی روی سطح سنگ از  $0^\circ$  قبل از پوشش دهی، به ترتیب به  $162^\circ$  و  $135^\circ$  درجه پس از پوشش دهی با نانوسیال افزایش یافتند. بعلاوه، پسماند زاویه تماس و همچنین زاویه ی لغزش آب روی سطح پوشش داده شده به ترتیب برابر  $0^\circ$  و  $<2^\circ$  اندازه گیری شد که نشان می‌دهد سنگ پس از پوشش دهی با این نانوسیال دارای خاصیت خودتمیزشوندگی شده است. مشخصه‌یابی سطح سنگ به وسیله ی آنالیزهای SEM، SP و EDX نشان داد که زبری نانوکامپوزیت  $ZnO/SiO_2$  با مورفولوژی ترکیبی شامل نانوصفحات و نانوذرات کروی، به همراه انرژی سطحی پایین مواد حاوی فلئور سبب بوجود آمدن حالت ابر گاز دوستی در سنگ شده است. در ادامه، عملکرد این نانوسیال به منظور تغییر ترشوندگی مغزه‌ی کربناته از حالت شدیداً مایع دوست به حالت ابر گاز دوست تحت شرایط عملیاتی مخزن، با انجام آزمایش‌های جریان سیال در سیستم گاز/مایع از طریق تزریق تک فازی مایع به درون مغزه‌ی اشباع شده از گاز مورد مطالعه قرار گرفت. نتایج آزمایش‌ها نشان داد که تحرک پذیری مایع در هر دو سیستم گاز/آب نمک و گاز/میعانات گازی بطور قابل ملاحظه‌ای پس از تغییر ترشوندگی سنگ افزایش یافت.

واژگان کلیدی: گاز دوست - تغییر ترشوندگی - نانوسیال - نانوکامپوزیت  $ZnO/SiO_2$  - مخزن گاز میعانی - مایع گریز